JOURNAL OF BONE AND MINERAL RESEARCH
Volume 23, Number 11, 2008
Published online on June 30, 2008; doi: 10.1359/JBMR.080605
© 2008 American Society for Bone and Mineral Research

Overexpression of Bone Sialoprotein Leads to an Uncoupling of Bone Formation and Bone Resorption in Mice

Paloma Valverde,[1,2] Jin Zhang,[1,2] Amanda Fix,[1] Ji Zhu,[1,3] Wenli Ma,[3] Qisheng Tu,[1] and Jake Chen[1]

ABSTRACT: The purpose of this study was to determine the effects of bone sialoprotein (BSP) overexpression in bone metabolism in vivo by using a homozygous transgenic mouse line that constitutively overexpresses mouse BSP cDNA driven by the cytomegalovirus (CMV) promoter. CMV-BSP transgenic (TG) mice and wildtype mice were weighed, and their length, BMD, and trabecular bone volume were measured. Serum levels of RANKL, osteocalcin, osteoprotegerin (OPG), TRACP5b, and PTH were determined. Bone histomorphometry, von Kossa staining, RT-PCR analysis, Western blot, MTS assay, in vitro mineralization assay, and TRACP staining were also performed to delineate phenotypes of this transgenic mouse line. Compared with wildtype mice, adult TG mice exhibit mild dwarfism, lower values of BMD, and lower trabecular bone volume. TG mice serum contained increased calcium levels and decreased PTH levels, whereas the levels of phosphorus and magnesium were within normal limits. TG mice serum also exhibited lower levels of osteoblast differentiation markers and higher levels of markers, indicating osteoclastic activity and bone resorption. H&E staining, TRACP staining, and bone histomorphometry showed that adult TG bones were thinner and the number of giant osteoclasts in TG mice was higher, whereas there were no significant alterations in osteoblast numbers between TG mice and WT mice. Furthermore, the vertical length of the hypertrophic zone in TG mice was slightly enlarged. Moreover, ex vivo experiments indicated that overexpression of BSP decreased osteoblast population and increased osteoclastic activity. Partly because of its effects in enhancing osteoclastic activity and decreasing osteoblast population, BSP overexpression leads to an uncoupling of bone formation and resorption, which in turn results in osteopenia and mild dwarfism in mice. These findings are expected to help the development of therapies to metabolic bone diseases characterized by high serum level of BSP.
J Bone Miner Res 2008;23:1775–1788. Published online on June 30, 2008; doi: 10.1359/JBMR.080605

Key words: bone sialoprotein, transgenic mouse, osteoclast, osteoblast, bone coupling

INTRODUCTION

There are three major ways in which bone may be formed or modified: osteogenesis, modeling, and remodeling. Osteogenesis is the initiation of bone formation on soft fibrous tissues (intramembranous ossification) or cartilage (endochondral ossification) during embryonic development or at the sites of injury. Modeling occurs after initial bone formation is established when large changes in the bone shape and structure are needed to adapt to the rapid growth in childhood. During this process, bone formation and bone resorption occur at different locations and the bone morphology is altered.[1] In contrast, remodeling occurs on existing bone surfaces but does not cause large changes in bone structure at a given site. During bone remodeling, bone resorption and bone formation are in a homeostatic equilibrium. Although old bone tissue is continuously replaced by new bone, there are no changes in bone morphology.[2] During the processes of both modeling and remodeling, it is important to maintain a certain balance between bone resorption by osteoclasts[3] and bone formation by osteoblasts[4] to achieve either normal bone development or bone homeostasis. A variety of cytokines, extracellular matrix proteins, and hormones have been shown to regulate osteoclastic and/or osteoblastic activities. Among these factors, RANKL, its cellular receptor, RANK, and the decoy receptor, osteoprotegerin (OPG), have been identified as the key regulators of physiological and pathological bone remodeling.[5–12] On binding to its receptor RANK in osteoclasts, RANKL induces osteoclast differentiation and activation, which in turn increases bone resorption.[6–12] In contrast, OPG inhibits bone resorption by osteoclasts through negatively regulating the binding between RANKL and RANK.[5] A higher ratio of RANKL-to-OPG has been associated with a variety of bone diseases characterized by excessive bone loss, which include postmenopausal osteoporosis, rheumatoid arthritis, periodontal disease, or tumor-associated bone loss.[9–12] Therapeutic inhibition of excessive bone resorption in these patients and in some animal models for these pathologies has been re-

The authors state that they have no conflicts of interest.

[1]Division of Oral Biology, Department of General Dentistry, Tufts University School of Dental Medicine, Boston, Massachusetts, USA; [2]These authors contribute equally to this work; [3]Institute of Genetic Engineering, South Medical University, Guangzhou, China.

ported on administration of a RANKL antibody or by downregulating the ratio of RANKL-to-OPG expression levels.[9–12]

Bone sialoprotein (BSP) is a major noncollagenous extracellular matrix protein in bone produced by osteoclasts, osteoblasts, osteocytes, and hypertrophic chondrocytes.[13–16] In vitro studies have suggested that BSP may function at several steps in bone modeling and remodeling. In addition to its ability to nucleate hydroxyapatite crystal formation and promote mineralization,[17,18] BSP was also reported to induce cell adhesion[19,20] and increase osteoclastogenesis and bone resorption.[21–24] Furthermore, although BSP expression is coincident with de novo bone formation[14,15] and ectopic calcification,[25–27] high BSP level in serum under pathological conditions has been associated with excessive bone resorption. For example, BSP expression was detected in many malignant tumor cells with a tendency of metastasis to bone and high serum BSP level was reported in patients suffering from osteotropic cancers and tumor-associated bone loss.[25,28–33] Several metabolic bone diseases characterized by excessive bone resorption, including postmenopausal osteoporosis, Paget's disease, ankylosing spondylitis, and rheumatoid arthritis have also been associated with abnormally high BSP level in serum or synovial fluid.[34–37] In contrast, treatments aimed at reducing excessive bone loss in postmenopausal women or patients with Paget's disease have been reported to decrease serum BSP level.[38,39] Although BSP expression in soft tissues and high serum BSP level are apparently associated with ectopic calcification and pathological bone remodeling, the effects of BSP overexpression in a transgenic mouse model remain unclear. In this study, we developed a transgenic mouse line that constitutively overexpresses BSP to investigate the effects of excessive BSP level on bone modeling and remodeling in vivo.

MATERIALS AND METHODS

Generation of CMV-BSP transgenic mice

Full-length murine BSP cDNA was subcloned into pRc/CMV vector (Invitrogen). The 2310-bp transgene fragment was cleaved out from the resulted CMV-BSP plasmid and microinjected into CB6F1 mouse embryos. Southern hybridization using tail DNA confirmed the integration of the transgene into the mouse genome, and slot blot analysis was performed to identify homozygous transgenic mice (named as CMV-BSP transgenic mice, data not shown). PCR was also performed to confirm the presence of the transgene. Mice were maintained and used in accordance with recommendations in the Guide for the Care and Use of Laboratory Animals prepared by the Institute on Laboratory Animal Resources, National Research Council (DHHS Publ. NIH 86–23, 1985) and by guidelines established by the Institutional Animal Care and Use Committee of the Tufts-New England Medical Center (Boston, MA, USA).

Structural parameters determination, DXA bone densitometry, μCT assay, and dry ash bone weight of femurs

CMV-BSP mice and wildtype mice were weighed (g), and their body length (nose-to-anus distance) and tail length (anus-to-tip of tail distance) were measured (mm) at 4 days, 4 wk, and 8 wk after birth. Mice were also autoradiographed using a Faxitron X-Ray MX-20 (Faxitron X-ray, Wheeling, IL, USA). Areal BMD (aBMD) of femurs and lumbar vertebral bones was assessed by DXA in 8-wk-old animals using a LUNARPIXIMUS densitometer (Lunar, Madison, WI, USA). The femurs from 8-wk-old CMV-BSP and wildtype mice were also scanned by μCT on a GE eXplore Locus Micro CT scanner. The following parameters were measured: bone volume, bone surface, and surface-to-volume ratio. At a 3D level, the following calculations were made as previously published[40]: relative bone volume over total bone volume (BV/TV), trabecular number (Tb.N), trabecular thickness (Tb.Th), and trabecular separation (Tb.Sp). The diameter of spheres filling the structure was taken as Tb.Th, the thickness of the marrow spaces as Tb.Sp, and the inverse of the mean distances of the skeletal structure was calculated as Tb.N. To determine the dry ash weight, the femurs were collected from 4-day- to 8-wk-old mice, and longitudinal length of the femurs was measured. Bones were placed in tared silica crucibles in a Barnstead/Thermolyne muffle furnace, dried to a constant weight at 110°C, and incinerated at 600°C for 48 h. Results were expressed as a ratio of ash weight to dry weight as a measurement of mineralization.[41,42]

Serum biochemistries

Blood samples were allowed to clot for 2 h and centrifuged at 3000 rpm for 10 min at room temperature. Serum was separated from the clot and frozen at –70°C. Levels of RANKL, osteocalcin (OC), OPG, TRACP5b, and PTH in serum were determined by ELISA with a Quantikine M mouse RANKL immunoassay kit (R&D Systems), a mouse osteocalcin EIA kit (Biomedical Technologies), an OPG ELISA kit (ALPCO; Diagnostics), a mouse TRACP5b ELISA kit (IDS), and the mouse intact PTH EIA, respectively. Levels of calcium, phosphorus, magnesium, and alkaline phosphatase (ALP) activity in serum were measured by colorimetric assays with a QuantiChromTM Calcium assay kit, a QuantiChromTM Phosphate assay kit, a QuantiChromTM Magnesium assay kit, and a QuantiChromTM ALP assay kit from BioAssay Systems, respectively (Hayward, CA, USA).

H&E staining, von Kossa staining, and TRACP histochemistry

Bone and soft tissues isolated from 4-day-, 6-wk-, and 8-wk-old CMV-BSP and wildtype mice were weighed (g) and fixed in 10% formalin for 24 h. Bone tissues were decalcified in 10% EDTA (pH 7.4) for 14 days at 4°C and equilibrated in PBS at 4°C for 1 day to remove the EDTA. All the bone and soft tissues were dehydrated in an ascending series of ethanol, cleared in xylene, and embedded in paraffin. Tissue sections, 6 μm in thickness, were mounted on glass slides, and H&E staining was performed. Ectopic calcification was monitored with a von Kossa stain kit from Diagnostic BioSystems by following the manufacturers' instructions (Pleasanton, CA, USA). Briefly, well-fixed paraffin-embedded soft tissues isolated from CMV-BSP mice

and wildtype mice were cut at 6 μm, and deparaffinized slides were hydrated through alcohols. After rinsed with distilled water, the slides were treated in 5% Silver Nitrate for 60 min with exposure to an UV light. The slides were rinsed with distilled water, treated in 5% sodium thiosulfate for 2–3 min, and stained with Nuclear Fast Red Stain for 5 min. The slides were dehydrated, cleared, mounted in paramount (Fisher Scientific), and microscopically examined. To quantify the number of TRACP-stained osteoclasts in vivo, TRACP staining was performed as previously described.[43] Briefly, femurs isolated from 10-wk-old CMV-BSP and wildtype mice were fixed in 10% formalin for 24 h and decalcified in 10% EDTA (pH 7.4) for 14 days at 4°C. Serial sections, 6 μm thick, were prepared and mounted on glass slides. The sections were stained for TRACP activities using a leukocyte acid phosphatase staining kit according to the manufacturer's instruction (Sigma). After incubation for 1 h at 37°C, the sections were counterstained with methyl green.

Bone histomorphometry

After H&E staining and TRACP staining, digital images were taken with a Nikon Eclipse E600 microscope and analyzed by Spot Advanced software (Diagnostic Instruments, Sterling Hights, MI, USA). In the trabecular area of the femoral epiphyses, the percentage of bone surface covered by cuboidal osteoblast (Ob.S/BS) and the ratio of osteoblast number to bone surface (Ob.N/BS, N/mm) were obtained from H&E-stained sections at 400-fold magnification. In the same area for bone resorption parameters, the percentage of trabecular osteoclast surface to bone surface (Oc.S/BS, %) and the ratio of osteoclast number to bone surface (Oc.N/BS, N/mm) were obtained from the measurement of TRACP-stained sections at 200-fold magnification. H&E-stained sections were also used to determine calvarial thickness and proximal tibial growth plate parameters. Measurements included determination of growth plate vertical height (top of resting zone to bottom of calcified cartilage), growth plate width (the width of the horizontal plane through the middle section of the growth plate), and the height of the zone occupied by hypertrophic chondrocytes and proliferative chondrocytes. The measurements of the growth plate height were performed in the central two thirds of the growth plate sections and were measured at equally spaced intervals parallel to the chondrocyte columns using SPOT Advanced Image software (Diagnostic Instruments). The total number of columns in the growth plate was also counted. Column density was expressed as the number of columns per millimeter of growth plate. For all samples, measurements were made on two nonconsecutive sections, and columns were defined as being composed of at least five chondrocytes. The number of proliferative and hypertrophic cells were counted in 10 longitudinal columns per growth plate and averaged for each growth plate (proliferative chondrocytes were defined by a height of <6 μm, whereas hypertrophic chondrocytes were defined by a height of >6 μm).

RT-PCR analysis

Freshly isolated RNA was reverse transcribed with a SuperScript first-strand synthesis kit (Invitrogen, Carlsbad, CA, USA), and the resulting cDNA was amplified using the Platinum PCR supermix (Invitrogen). The sequences of the primers for amplification of mouse BSP were 5′-GGAGGGGGCTTCACTGAT-3′ and 5′-AACAATCC-GTGCCACCA-3′ and for mouse GAPDH were 5′-ATC-ACTGCCACCCAGAAGAC-3′ and 5′-ATGAGGTC-CACCACCCTGTT-3′. Images of the amplified products in 1% agarose gels were captured with an UVP Bioimaging system and processed by Adobe Photoshop 6.0 (Adobe Systems, San Jose, CA, USA) and Scion Image Beta 4.02 (Scion Image, Frederick, MD, USA). GAPDH amplification was performed for normalization purposes.

Western blot analysis

Western blot analysis and image quantification were performed essentially as described.[21] Two different anti-BSP antibodies were used with comparable results (data not shown): a rabbit anti-human BSP antibody (1:2500) against the full-length human recombinant protein (Chemicon, Temecula, CA, USA) and a rabbit anti-human BSP antibody (1:200) against a peptide containing amino acids 108–122 of the human protein (ALPCO). Results shown in this manuscript were obtained with the anti-BSP antibody from Chemicon. Before Western blot analysis, serum samples from wildtype and CMV-BSP mice were concentrated five times with Microcon centrifugal YM-30 filter devices from Millipore (Bedford, MA, USA). Analysis was performed with at least three serum samples per time point, and known amounts of recombinant human BSP (ALPCO) were also used as control. Mouse anti-GAPDH antibody (Santa Cruz Biotechnologies, Santa Cruz, CA, USA) or mouse anti-β actin antibody (Sigma) were used for normalization. The secondary antibodies were horseradish peroxidase (HRP)-linked goat-anti rabbit IgG (US Biological, Swampscott, MA, USA) or HRP linked goat-anti mouse IgG secondary antibody (Abcam, Cambridge, MA, USA). Blots were visualized using ECL chemiluminescence reagents from Pierce Biotechnology (Rockford, IL, USA).

MTS assays of calvarial cells and macrophage-colony stimulating factor–treated bone marrow–derived monocytes/macrophages cells

Murine osteoclast precursor cells in the form of bone marrow–derived monocytes/macrophages (BMMs) and murine osteoblast precursor cells in the form of calvarial cells were isolated from 6- to 8-wk-old mice as previously described.[21,44] Cells were cultured at a density of 3000 viable cells/well on 96-well plates, and the number of viable cells was determined by the CellTiter 96 Aqueous nonradioactive cell proliferation assay (MTS assay; Promega, Madison, WI, USA). In these assays, calvarial cells were cultured in α-MEM supplemented with 10% heat-inactivated FBS (HIFBS), 2 mM L-glutamine, 100 U/ml penicillin, and 100 μg/ml streptomycin, whereas BMM cells were cultured in α-MEM supplemented with 10% HIFBS, 2 mM L-glutamine, 100 U/ml penicillin, 100 μg/ml strepto-

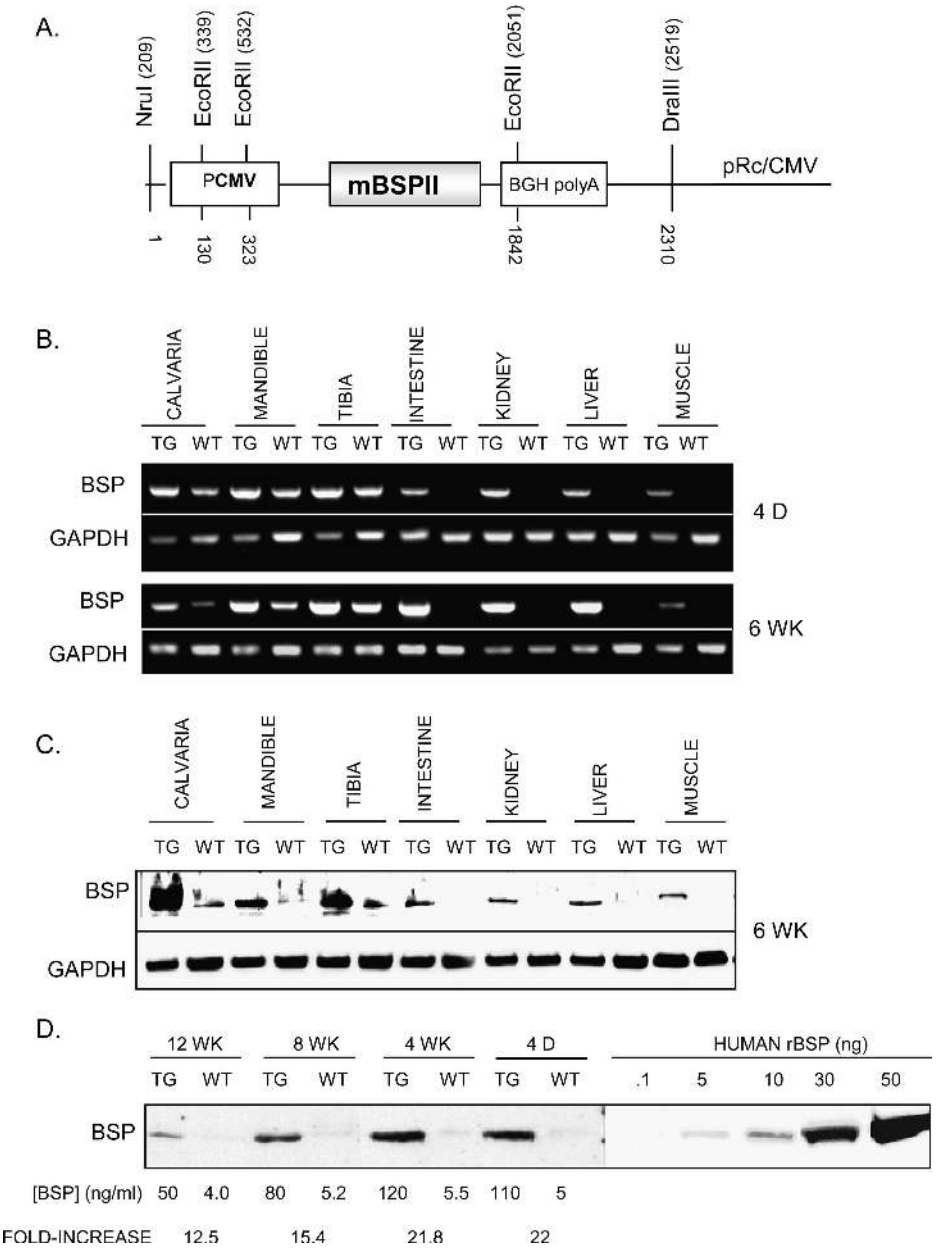

FIG. 1. Generation of a homozygous CMV-BSP transgenic mouse line that exhibits constitute overexpression of BSP. (A) Map of CMV-BSP transgenic construct. (B(RT-PCR analysis of BSP and GAPDH expression levels in soft and mineralized tissues of 4-day-old (4D) and 6-wk-old (6 WK) wildtype (WT) and CMV-BSP transgenic (TG) mice. (C) Western blot analysis of BSP expression in different tissues of 6-wk-old (6 WK) CMV-BSP transgenic and wildtype mice. Immunoreaction for GAPDH was used as a loading control. Experiments shown in B and C were performed three times with similar results. (D) Western blot analysis of BSP in serum of CMV-BSP transgenic and wildtype mice at 6 wk after birth. Estimation of the levels of BSP in serum of CMV-BSP and wildtype mice was performed by comparing the immunoreaction obtained with serum samples and with known amounts of human recombinant BSP (human rBSP, ALPCO). Serum samples were collected from 4-day-old (4D), 4-wk-old (4 WK), 8-wk-old (8 WK), and 12-wk-old (12 WK) mice. Results of BSP concentration in serum are expressed as the mean of three different experiments performed with different serum samples. Fold-increase is defined as the increase in BSP levels in TG vs. WT.

mycin, and 10 ng/ml macrophage-colony stimulating factor (M-CSF; Peprotech, Rocky Hill, NJ, USA). The quantity of formazan product that is directly proportional to the number of viable cells was measured by the absorbance at 405 nm.

In vitro osteogenic differentiation and mineralization of calvarial cultures

For in vitro osteogenic differentiation, confluent calvarial cells were treated with 10 nM dexamethasone and 50 μg/ml of ascorbic acid. β-glycerophosphate (10 mM) was added after nodules formed 2 wk later. Quantitative determination of ALP was performed in cell lysates by colorimetric assay of enzyme activity using an ALP kit from BioAssay system (Hayward, CA, USA) as recommended by the manufacturer. The optical density of the yellow product paranitrophenol was determined spectrophotometrically at 405 nm. Protein concentration of the cell lysates was measured with a BCA Protein Assay Kit (Pierce, Rockford, IL, USA), and ALP activity was expressed as paranitrophenol produced in nmol/min/mg of protein. Detection and quantification of bone nodule formation was performed by alizarin red-S histochemical staining. Briefly, cells were fixed with 4% phosphate-buffered formalin and rinsed three times with water. Cells were treated with a 2% (weight/volume) solution of Alizarin red-S stain at pH 4.0 (Sigma, St Louis, MO, USA) for 10 min and washed with 1× PBS for 15 min with gentle agitation. Digital images of the different stainings were taken at ×10 magnification. Bone nod-

TABLE 1. STRUCTURAL PARAMETERS, BMD, AND BMC OF MALE (M) AND FEMALE (F) WILDTYPE (WT) AND CMV-BSP TRANSGENIC MICE (TG)

	4 days old		*4 wk old*				*8 wk old*			
			WT		*TG*		*WT*		*TG*	
	WT	*TG*	*M*	*F*	*M*	*F*	*M*	*F*	*M*	*F*
Body weight (g)	2.7 ± 0.1	2.9 ± 0.2	15.1 ± 0.6	11.7 ± 0.5*	12.8 ± 0.5†	9.9 ± 1.1†	23.3 ± 1.3	18.5 ± 0.7*	17.4 ± 0.4†	15.3 ± 1.0†
Body length (mm)	40.1 ± 1.4	40.6 ± 1.1	75.8 ± 1.6	75.5 ± 1.2	68.6 ± 1.4†	68.7 ± 1.8†	88.0 ± 1.4	82.0 ± 1.6	81.5 ± 1.8†	75.2 ± 2.0†
Tail length (mm)	17.5 ± 0.7	16.3 ± 0.6	59.2 ± 0.5	58.5 ± 1.0	52.4 ± 1.5*	50.3 ± 0.7†	77.0 ± 0.9	76.4 ± 0.5	69.5 ± 0.6†	69.0 ± 0.8†
Femur length (mm)	3.3 ± 0.3	3.2 ± 0.1	11.1 ± 0.4	10.9 ± 0.3	9.8 ± 0.2†	9.9 ± 0.1†	15.2 ± 0.2	13.9 ± 0.2	13.8 ± 0.3†	13.0 ± 0.3†
BMD (g/cm^2) (DXA)										
Femoral	n.t.	n.t.	n.t.	n.t.	n.t.	n.t.	0.079 ± 0.002	0.074 ± 0.002	0.071 ± 0.002†	0.059 ± 0.003†
Vertebral	n.t.	n.t.	n.t.	n.t.	n.t.	n.t.	0.073 ± 0.002	0.071 ± 0.001	0.062 ± 0.003†	0.059 ± 0.002†
BMD (mg/ml) (μCT)										
Femoral	n.t.	n.t.	n.t.	n.t.	n.t.	n.t.	n.t.	22.68 ± 2.28	n.t.	16.13 ± 1.07†
BV/TV (%)	n.t.	n.t.	n.t.	n.t.	n.t.	n.t.	n.t.	65.23 ± 3.05	n.t.	52.25 ± 2.76†
Tb.Th (μm)	n.t.	n.t.	n.t.	n.t.	n.t.	n.t.	n.t.	178 ± 10.67	n.t.	133 ± 6.87†
Tb.N (mm^{-1})	n.t.	n.t.	n.t.	n.t.	n.t.	n.t.	n.t.	3.15 ± 0.012	n.t.	1.69 ± 0.011†
Tb.Sp (μm)	n.t.	n.t.	n.t.	n.t.	n.t.	n.t.	n.t.	174 ± 7.25	n.t.	245 ± 12.21†
Bone ash (% dry weight)	30.4 ± 1.6	32.3 ± 1.2	53.1 ± 1.1	51.9 ± 0.8	41.3 ± 1.3†	38.5 ± 1.2†	58.8 ± 1.7	56.2 ± 0.8	43.0 ± 1.8†	42.5 ± 1.4†

The data are the mean ± SE for groups of 5–10 mice.

* $p < 0.01$, M vs. F mice of the same genotype.

† $p < 0.01$, TG vs. WT mice of same sexr and age.

n.t., not tested.

ule number was counted in six different fields of each well and in three independent experiments.

Assessment of number of TRACP$^+$ multinucleated cells and bone resorption in vitro

Osteoclast differentiation and bone resorption pits were identified and quantified essentially as previously described,[21] with minor modifications. Briefly, red-stained TRACP$^+$ cells with 5 or less nuclei and 10 or more nuclei (multinucleated cells [MNCs]) were identified using the K-ASSAY TRACP staining kit from Kamiya Biomedical Company (Seattle, WA, USA) in BMM cultures from wildtype and CMV-BSP mice treated with 10 ng/ml M-CSF and 50 ng/ml RANKL for 5 or 9 days. Digital images were analyzed with a Nikon Eclipse E600 microscope and Spot Advanced software. Results were expressed as TRACP$^+$ MNCs per well. To evaluate bone resorption pit formation, cultures were performed on hydroxyapatite discs (BD BioCoat Osteologic; BD Biosciences, Ontario, Canada) or dentin discs (ALPCO) for 7 days as previously described.[21] To measure the areas of resorption lacunae on the osteologic discs, cells were removed with domestic bleach, and digital images of the discs were taken under dark-field microscopy with a Nikon Eclipse E600 microscope and Spot Advanced software. To measure the areas of resorption lacunae on the dentin discs, cells were removed with domestic bleach and discs were stained with 1% toluidine blue in 0.5% sodium tetraborate solution for 10 minutes and photographed under brightfield microscopy. Resorbed area on the digital images of osteologic or dentin discs were measured with the Scion Image Beta 4.02 software (Scion, Frederick, MD, USA) and expressed as percent resorbed area = (resorbed area per disc/total disc area) × 100.

Statistical analysis

Generally results are shown as the mean ± SE of the number of experiments or number of mice except those specifically indicated in the legends. One-way ANOVA was used to test significance using the software package Origin 6.1 (OriginLab, Northampton, MA, USA). Values of $p < 0.01$ or 0.05, as specifically indicated in the legends, were considered statistically significant.

RESULTS

CMV-BSP transgenic mice express BSP constitutively

To determine the effects of high BSP expression levels on bone metabolism in vivo, a homozygous transgenic mouse line was created in which constitutive mouse BSP overexpression was driven by the CMV promoter (Fig. 1A, CMV-BSP mice). Semiquantitative RT-PCR (Fig. 1B) and Western blot analyses (Fig. 1C) confirmed that BSP expression levels in mineralized tissues isolated from CMV-BSP mice were higher than those from wildtype mice. Furthermore, BSP expression was detected in all soft tissues isolated from CMV-BSP mice. Additional Western blot analyses were performed to estimate the levels of intact BSP in concentrated serum samples of CMV-BSP and wildtype mice by comparison with known concentrations of recombinant BSP (Fig. 1D). Because of the unavailability of mouse recombinant BSP for these studies, human recombinant BSP was used as a standard, and therefore the absolute levels of BSP calculated using this method should be considered as a rough estimate. Based on this estimated analysis, BSP was found within the range of 50–120 ng/ml in serum samples of CMV-BSP mice and ~5 ng/ml in those from wildtype mice (Fig. 1D). Although intact BSP level in serum was significantly higher in CMV-BSP mice than in wildtype mice at all ages studied (Fig. 1D), it was significantly decreased in serum samples from 8- and 12-wk-old mice compared with those from younger mice (4-day- or 4-wk-old mice; Fig. 1D).

Adult CMV-BSP transgenic mice exhibit mild dwarfism, a lack of ectopic calcification, lower values of BMD, and lower trabecular bone volume compared with wildtype mice

To evaluate the effects of BSP overexpression on gross skeletal phenotypes, structural parameters were monitored in wildtype and CMV-BSP mice at different ages. At 4 days after birth, no difference in body weight was detected between CMV-BSP and wildtype mice. In contrast, the body weight of CMV-BSP mice at 4 and 8 wk of age was lower than that of the wildtype mice, which indicated a retardation of postnatal development resulted from BSP overexpression (Table 1). Longitudinal skeletal growth was also altered in transgenic mice at 4 and 8 wk of age, as indicated by their lower body, tail, and femur lengths (Table 1). DXA results indicated that both femoral and lumbar vertebral areal BMD was reduced in CMV-BSP mice compared with wildtype mice (Table 1). μCT scan analysis also showed a decreased BMD (28.88%) in CMV-BSP mice compared with wildtype mice. The total trabecular volume (BV/TV) in CMV-BSP mice was decreased by 19.89%, and the trabecular number (Tb.N) decreased by 46.35% compared with the wildtype mice. Trabecular thickness (Tb.Th) was 25.28% lower in CMV-BSP mice than in wildtype mice, whereas trabecular separation (Tb.Sp) was increased by 40.80% in CMV-BSP mice compared with wildtype mice (Table 1). Mineral content determined as the percentage of femoral ash weight to dry weight was significantly decreased in CMV-BSP mice at 4 and 8 wk of age but not at 4 days after birth (Table 1). The weights of different soft tissues including heart, lung, liver, kidney, and brain were not significantly different between wildtype and CMV-BSP mice at the 4-day, 6-wk, and 8-wk time points (data not shown). We were not able to find soft tissue mineralization in either CMV-BSP or wildtype mice (up to 8 wk of age, data not shown) by whole body X-ray, soft tissue X-ray, or von Kossa stainings.

CMV-BSP mice exhibit a downregulation in serum markers of osteoblastic function and an upregulation in markers of osteoclastic activity compared with wildtype mice

We next measured the levels of several markers of bone remodeling and of calcium/phosphate homeostasis in the

TABLE 2. SEROLOGY OF MARKERS OF BONE REMODELING AND CALCIUM/PHOSPHATE HOMEOSTASIS REGULATION IN MALE (M) AND FEMALE (F) WILDTYPE (WT) AND TRANSGENIC MICE (TG)

	4 days old		*4 wk old*				*8 wk old*			
			WT		*TG*		*WT*		*TG*	
	WT	*TG*	*M*	*F*	*M*	*F*	*M*	*F*	*M*	*F*
PTH (pg/ml)	12 ± 1.5	6.5 ± 1.0*	20.1 ± 1.9	22.4 ± 2.0	15.4 ± 0.5*	13.0 ± 3.0*	25.3 ± 2.0	26.0 ± 2.2	19.2 ± 2.5*	20.5 ± 2.1*
Calcium (mg/dl)	6.8 ± 0.4	10.5 ± 0.3*	6.1 ± 0.5	6.5 ± 0.6	10.1 ± 0.2*	9.8 ± 0.2*	6.5 ± 0.6	6.2 ± 0.4	9.1 ± 0.5*	10.2 ± 0.7*
Phosphorus (mg/dl)	10 ± 0.9	10.6 ± 0.7	8.6 ± 0.4	8.0 ± 0.6	9.0 ± 0.6	7.9 ± 0.5	7.8 ± 0.3	7.6 ± 0.5	7.9 ± 0.8	8.2 ± 0.4
Magnesium (mg/dl)	3.2 ± 0.3	3.5 ± 0.2	3.0 ± 0.2	3.2 ± 0.3	2.9 ± 0.3	3.0 ± 0.1	2.6 ± 0.3	2.5 ± 0.2	2.5 ± 0.2	2.6 ± 0.1
Osteocalcin (ng/ml)	525 ± 22	480 ± 19*	252 ± 12	245 ± 14	202 ± 16*	190 ± 10*	112 ± 15	125 ± 10	80 ± 15*	94 ± 15*
ALP (IU/liter)	394 ± 29	309 ± 26*	168 ± 15	156 ± 12	105 ± 12*	111 ± 9*	38 ± 4	40 ± 5	27 ± 4*	22 ± 3*
TRACP5b (U/liter)	3.8 ± 0.4	7.4 ± 0.5*	3.0 ± 0.3	5.5 ± 0.2†	5.4 ± 0.4*	13.5 ± 0.6*	3.2 ± 0.2	6.6 ± 0.6†	5.9 ± 0.3*	18.8 ± 1.2*
RANKL (pg/ml)	68 ± 9.0	109 ± 12*	101 ± 9.2	110 ± 12	148 ± 12*	176 ± 10*	174 ± 10	153 ± 18	272 ± 25*	232 ± 30*
OPG (ng/ml)	1.9 ± 0.2	1.4 ± 0.1*	1.5 ± 0.1	1.3 ± 0.2	0.9 ± 0.1*	0.8 ± 0.1*	1.2 ± 0.2	1.3 ± 0.2	0.5 ± 0.1*	0.6 ± 0.1*

The data are the mean ± SE for groups of 4–15 mice.
* $p < 0.01$, TG vs. WT mice of same sex and age.
† $p < 0.01$, M vs. F mice of the same genotype.

serum of wildtype and CMV-BSP mice. CMV-BSP mice showed significantly higher levels of calcium and lower levels of PTH than wildtype mice at 4 days, 4 wk, and 8 wk of age (Table 2). However, no changes in the levels of phosphate and magnesium were detected between the two groups at all the time points examined (Table 2). Together with serum ALP activity, serum OC level has long been used as a marker for osteoblast activity and new bone formation.[45,46] Our results showed that these markers of osteoblastic function were significantly lower in CMV-BSP mice than in the wildtype mice. In contrast, serum levels of active TRACP5b, an enzyme that is released from osteoclasts during bone resorption,[47] were significantly higher in CMV-BSP mice than in the wildtype mice. In addition, soluble RANKL levels were increased whereas levels of OPG were decreased in serum samples of CMV-BSP mice compared with those of wildtype mice.

Histomorphometric analysis of CMV-BSP mouse bones

Histological analysis of bone tissues from 4-day-, 6-wk- and 8-wk-old wildtype and CMV-BSP mice showed that calvarial bones derived from CMV-BSP mice were thinner than those from wildtype mice (Fig. 2). Histomorphometric analysis quantitatively confirmed these findings (Table 3). Mandibles of CMV-BSP mice were characterized by thinner supporting bone and more osteoclasts located in the molar root area (Fig. 2). No significant difference in the vertical length of proximal tibial growth plate was detected between CMV-BSP and wildtype mice (Table 3). However, compared with the wildtype mice, CMV-BSP mice exhibited an expanded hypertrophic zone with more layers of hypertrophic cells (Table 3), whereas in 8-wk-old CMV-BSP mice, the proliferative zone vertical length was decreased. Furthermore, the growth plate width was also decreased in 6- and 8-wk-old CMV-BSP mice compared with the wildtype controls (Table 3). In addition, the newly formed bone in secondary spongiosa showed a more porous pattern with enlarged bone marrow spaces and an increased number of multinucleated giant osteoclasts. Furthermore, the secondary calcification center of the tibia was characterized by the presence of bone tissue with osteoporotic features, including the presence of less bone trabeculae and numerous osteoclasts (Fig. 2). TRACP staining further confirmed the increased number of $TRACP^+$ osteoclasts in the trabecular area of the femoral epiphyses isolated from 10-wk-old CMV-BSP mice compared with the wildtype mice (Fig. 3A), as indicated by the results of Oc.N/BS (Fig. 3B) and Oc.S/BS (Fig. 3C). In the trabecular area of the femoral epiphyses, the percentage of bone surface covered by cuboidal osteoblast (Ob.S/BS) and the ratio of osteoblast number to bone surface (Ob.N/BS, N/mm) were also determined. However, no statistical significance in these osteoblastic parameters was observed between CMV-BSP mice and their control wildtype mice (Figs. 3D and 3E).

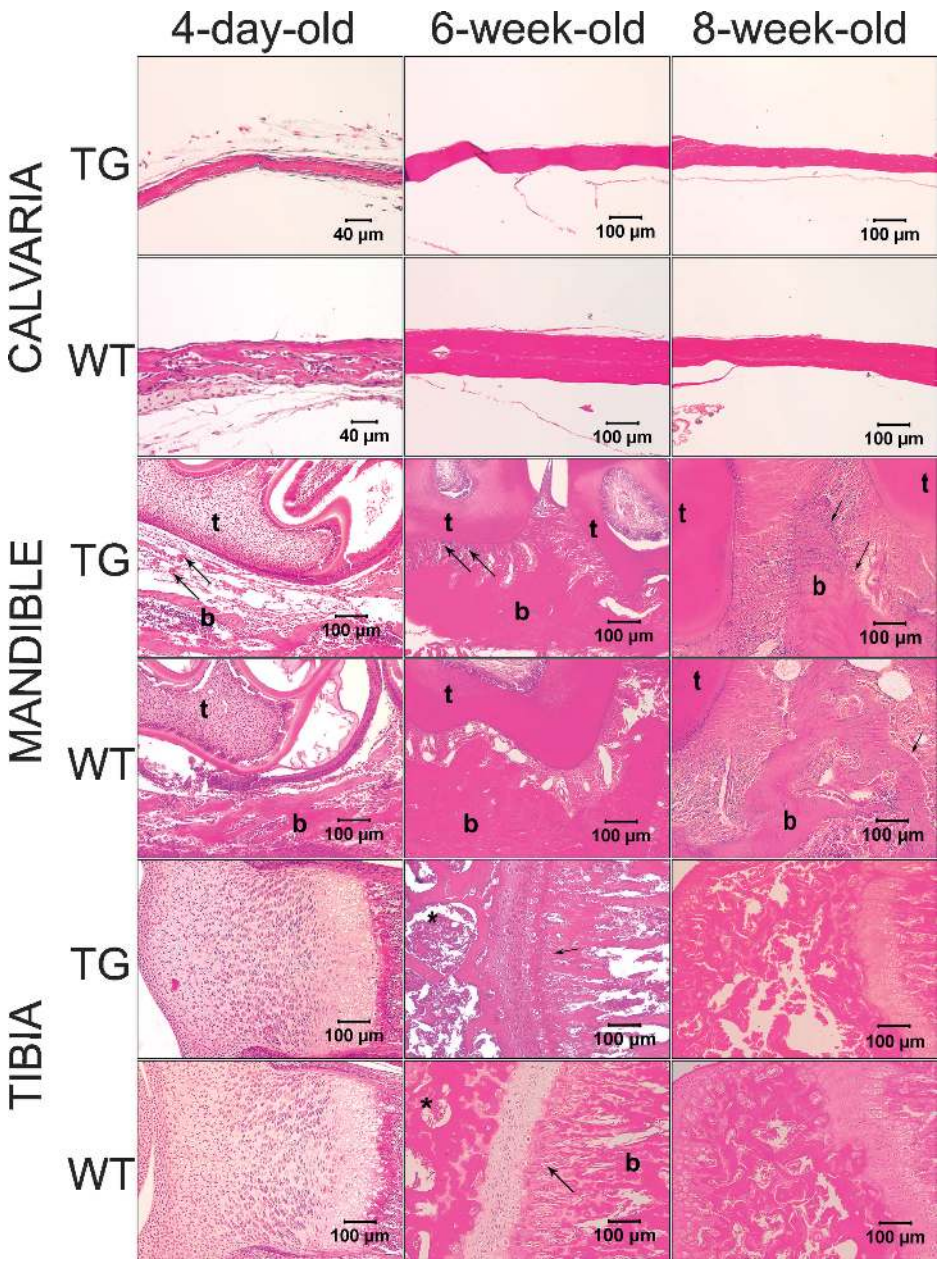

FIG. 2. H&E staining of bone tissues from CMV-BSP transgenic and wildtype mice. The calvarial bones of 4-day-old, 6-wk-old, and 8-wk-old CMV-BSP mice were thinner and less developed than those of wildtype mice. More reverse lines were seen, indicating a faster remodeling in CMV-BSP than in wildtype mice. Mandibular bone (b) in 4-day-old CMV-BSP mice was generally thinner than that in wildtype mice of the same age. Many osteoclasts were present in the root area of molar teeth (t) in 6-wk-old transgenic mice. The alveolar bone (b) that supported the tooth (t) attracted many osteoclasts (arrows) on its surface as can be seen in a representative 8-wk-old transgenic mouse. At the same location in a representative wildtype mouse, the alveolar bone (b) was lined up by osteoblasts (arrows). In the secondary spongiosa beneath the epiphyseal cartilage (arrows) of tibias of 6-wk-old transgenic mice, the newly formed bone showed a more porous pattern (b) and an increased number of multinucleated giant osteoclasts compared with those of wildtype mice. Enlarged bone marrow spaces (*) were present in secondary center of ossification of the tibia. In the secondary center of ossification of tibias from 8-wk-old CMV-BSP mice, bone tissue showed osteoporotic features including less bone trabeculae and the presence of numerous osteoclasts.

Ex vivo experiments to determine possible differences in osteoclastic activity between wildtype and CMV-BSP transgenic mice

BMM cells were cultured in the presence of M-CSF or M-CSF and RANKL to induce the proliferation or differentiation, respectively. Expression of BSP mRNA was ~2.5-fold higher in cultures established from transgenic mice than in those from wildtype mice under both experimental conditions (Fig. 4A). MTS assays indicated that in M-CSF–treated BMM cultures, the living cell numbers were similar in wildtype and CMV-BSP cultures (Fig. 4B). However, when BMM cells were induced to differentiate into osteoclasts by M-CSF and RANKL, the number of $TRACP^+$ MNCs was higher in cultures derived from the transgenic mice (Fig. 4C). The higher numbers of differentiated cells in transgenic cultures than in the wildtype cultures were observed both on day 5 and day 9 after the initiation of the treatment. Considering that large osteoclasts with 10 or more nuclei have been reported to resorb bone more efficiently in vitro than small osteoclasts with 5 or less nuclei,[48] we determined the numbers of $TRACP^+$ MNCs containing 5 or less nuclei and 10 or more nuclei, respectively. Our results showed that cell cultures derived from CMV-BSP mice contained increased number of larger osteoclasts compared with those from wildtype mice (Fig. 4C). In addition, M-CSF/RANKL-treated cells cultured on hydroxyapatite and dentin slices showed ~3-fold higher bone resorption area than those from the wildtype mice (Fig. 4D).

TABLE 3. HISTOMORPHOMETRIC ANALYSIS OF FEMALE WILDTYPE (WT) AND CMV-BSP TRANSGENIC MICE (TG)

	4 days old		6 wk old		8 wk old	
	WT	TG	WT	TG	WT	TG
Calvarial thickness (μm)	22.25 ± 4.37	18.25 ± 2.92*	126.70 ± 18.23	93.17 ± 11.85*	102.5 ± 12.43	82.22 ± 11.79*
Growth plate vertical length (μm)	808.67 ± 84.96	799.33 ± 78.67	127.03 ± 12.85	133.94 ± 14.43	120.17 ± 16.48	126.84 ± 15.84
Proliferative zone vertical length (μm)	550.12 ± 54.38	534.67 ± 51.78	77.42 ± 8.35	72.30 ± 6.93	74.29 ± 8.32	56.89 ± 5.63*
Proliferating cells per column (#/column)	n.t.	n.t.	7.67 ± 1.27	7.37 ± 1.52	6.50 ± 1.84	6.03 ± 1.20*
Hypertrophic zone vertical length (μm)	159.67 ± 12.33	194.33 ± 15.39*	42.43 ± 6.84	53.70 ± 5.92*	37.33 ± 5.84	50.67 ± 5.33*
Hypertrophic cells per column (#/column)	9.50 ± 1.91	13.67 ± 1.87*	3.83 ± 0.57	4.67 ± 0.67*	3.52 ± 0.37	4.33 ± 0.67*
Growth plate width (μm)	616.43 ± 58.91	618.95 ± 62.87	2515.83 ± 192.37	2324.49 ± 221.67*	2727.63 ± 319.28	2571.39 ± 290.07*
Column density (column #/mm)	53.83 ± 5.38	51.78 ± 6.11	54.88 ± 6.29	56.15 ± 7.13	45.98 ± 6.22	49.02 ± 5.73

The data are the mean ± SE for groups of 5–10 mice.
* $p < 0.05$, TG vs. WT mice.
n.t., not tested.

Ex vivo experiments to determine putative differences in osteoblastic functions between wildtype and CMV-BSP mice

Osteoblast precursor cells in the form of primary calvarial cell cultures were established from 4-day-old wildtype and transgenic mice. In both osteogenic medium and nonosteogenic medium, the expression of BSP mRNA was found to be significantly higher in cultures established from transgenic than in those from wildtype mice (Fig. 5A). In addition, as indicated by MTS assay, living cell number of transgenic calvarial cells cultured in nonosteogenic medium was lower than those obtained from WT mice (Fig. 5B). ALP activity, an early marker of osteoblastic differentiation,[49] was found to be significantly higher in cell lysates from transgenic cultures (Fig. 5C). Furthermore, on induction of osteogenic differentiation, calvarial cells from transgenic mice formed a higher number of mineralized bone nodules than those from wildtype mice (by 2.6-fold; Fig. 5D).

DISCUSSION

In this study, we described for the first time the effects of BSP overexpression on bone metabolism using a CMV-BSP transgenic mouse model in which constitutive BSP overexpression was driven by a CMV promoter. As a result of BSP overexpression in all the tissues of this mouse model, the serum levels of intact BSP in CMV-BSP mice were >10-fold higher than those in the wildtype mice. However, despite expression of BSP in all the soft tissues, no ectopic calcification was detected in the adult transgenic mice. Although some studies associated BSP with ectopic calcification,[25–27] recent reports have suggested that expression of BSP may not be sufficient to promote ectopic calcification.[50,51] These recent reports, together with our results that CMV-BSP mice lacks ectopic calcification, suggest that increasing the BSP level alone is not sufficient to induce ectopic calcification in the tissues that do not express BSP under physiological conditions (i.e., liver, kidney, periodontal ligament).

In our study, adult transgenic mice overexpressing BSP were characterized by their reduced aBMD and trabecular bone volume in femurs and lumbar vertebral bones compared with those in wildtype mice. This phenotype appeared to be, at least in part, caused by the effects of BSP overexpression in increasing bone resorption by increasing osteoclastic activity. In agreement with this hypothesis, we detected higher levels of the specific osteoclastic marker TRACP5b, higher RANKL to OPG ratio, and higher calcium in the serum of CMV-BSP mice than in that of wildtype mice. Furthermore, ex vivo studies with osteoclast precursor cells indicated that transgenic cultures differentiated more efficiently in the presence of RANKL and MCSF and exhibited an increased ability to resorb dentin or hydroxyapatite compared with wildtype cultures. These results were also consistent with our previous findings that human recombinant BSP and soluble RANKL act synergistically to increase bone resorption in vitro.[21] Moreover, in cell cultures treated by M-CSF and RANKL, we found that the

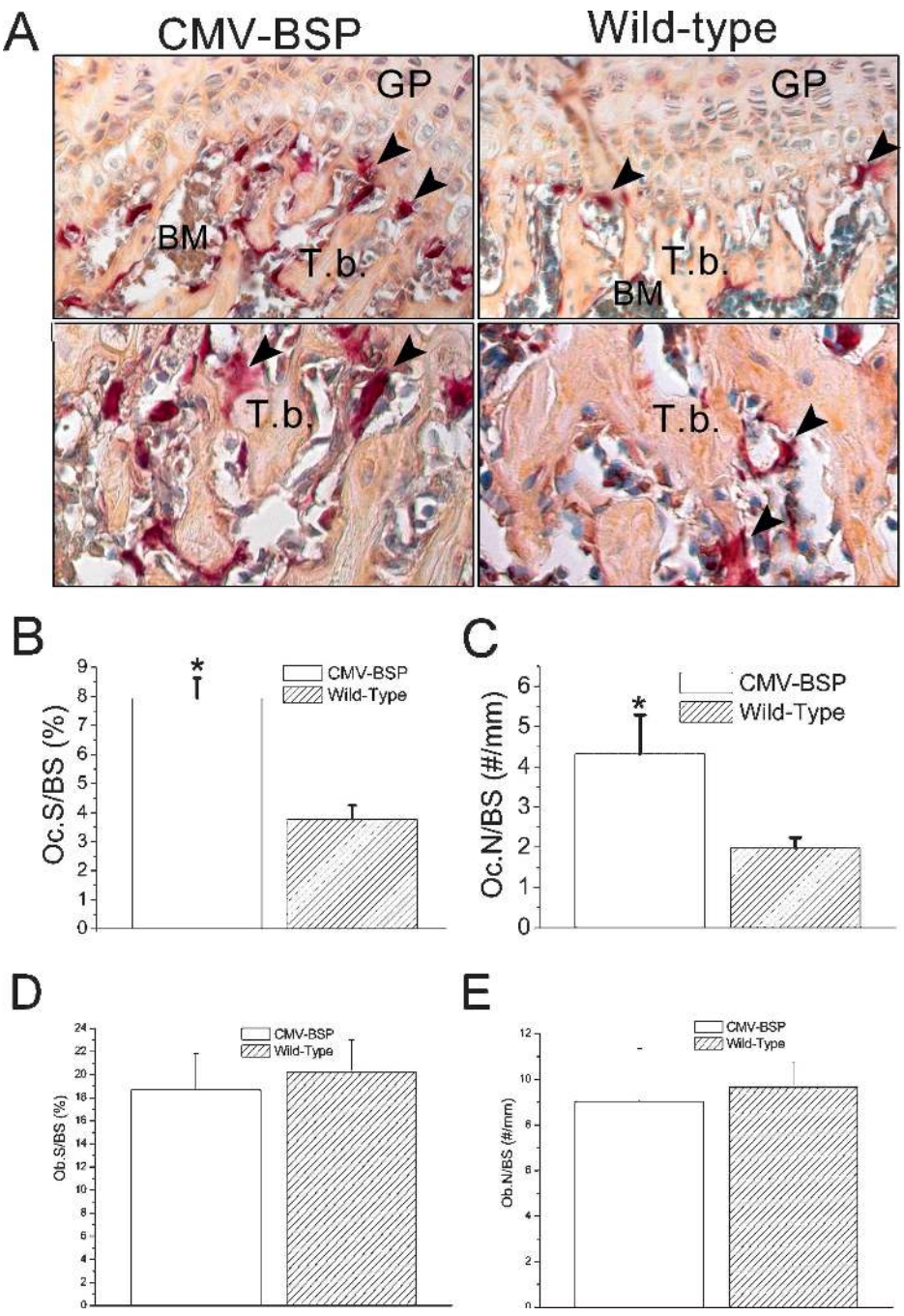

FIG. 3. TRACP staining showed an increased number of TRACP$^+$ osteoclasts in the trabecular area of the femoral epiphyses isolated from 10-wk-old CMV-BSP mice compared with the wildtype mice. (A) TRACP staining sections showed thinner trabecular bone and increased TRACP$^+$ osteoclasts in CMV-BSP group. GP, growth plate; T.b., trabecular bone; BM, bone marrow; arrowhead, TRACP$^+$ osteoblasts. Photographs were taken at ×40 magnification. (B and C) Bone area covered by bone-resorbing osteoclasts. Oc.S/BS, osteoclast surface/bone surface; Oc.N/BS, osteoclast number/bone surface. (D and E) Bone area covered by cuboidal osteoblasts. Ob.S/BS, osteoblast surface/bone surface; Ob.N/BS, osteoblast number/bone surface. Data are presented as mean ± SE of four different samples (*$p < 0.05$, CMV-BSP vs. wildtype).

amount of large osteoclasts with 10 or more nuclei was higher in transgenic cultures than in wildtype cultures. As indicated by several in vivo and in vitro studies, large osteoclasts with 10 or more nuclei are more active bone resorbers than small osteoclasts with 5 or less nuclei.[48,52–54] Other in vivo bone resorption parameters, the percentage of trabecular osteoclast surface to bone surface (Oc.S/BS, %) and the ratio of osteoclast number to bone surface (Oc.N/BS, N/mm) were also increased in transgenic mice compared with those in wildtype mice, which further confirmed the ability of BSP to increase osteoclastic activity and bone resorption in vivo.

In our study, we also found that living cell number of transgenic calvarial cells cultured in nonosteogenic medium was lower than those obtained from WT mice, the reason for which could be a lower proliferation rate and a higher apoptosis rate. The reduced living calvarial cell number observed in BSP overexpressing cell cultures seemed to be coupled with an accelerated osteogenic differentiation as indicated by the higher ALP activity of transgenic cultures. Our results suggested that transgenic-derived calvarial cell cultures were characterized by a more differentiated phenotype compared with cells derived from wildtype mice. Osteoblastic cultures from transgenic mice also exhibited

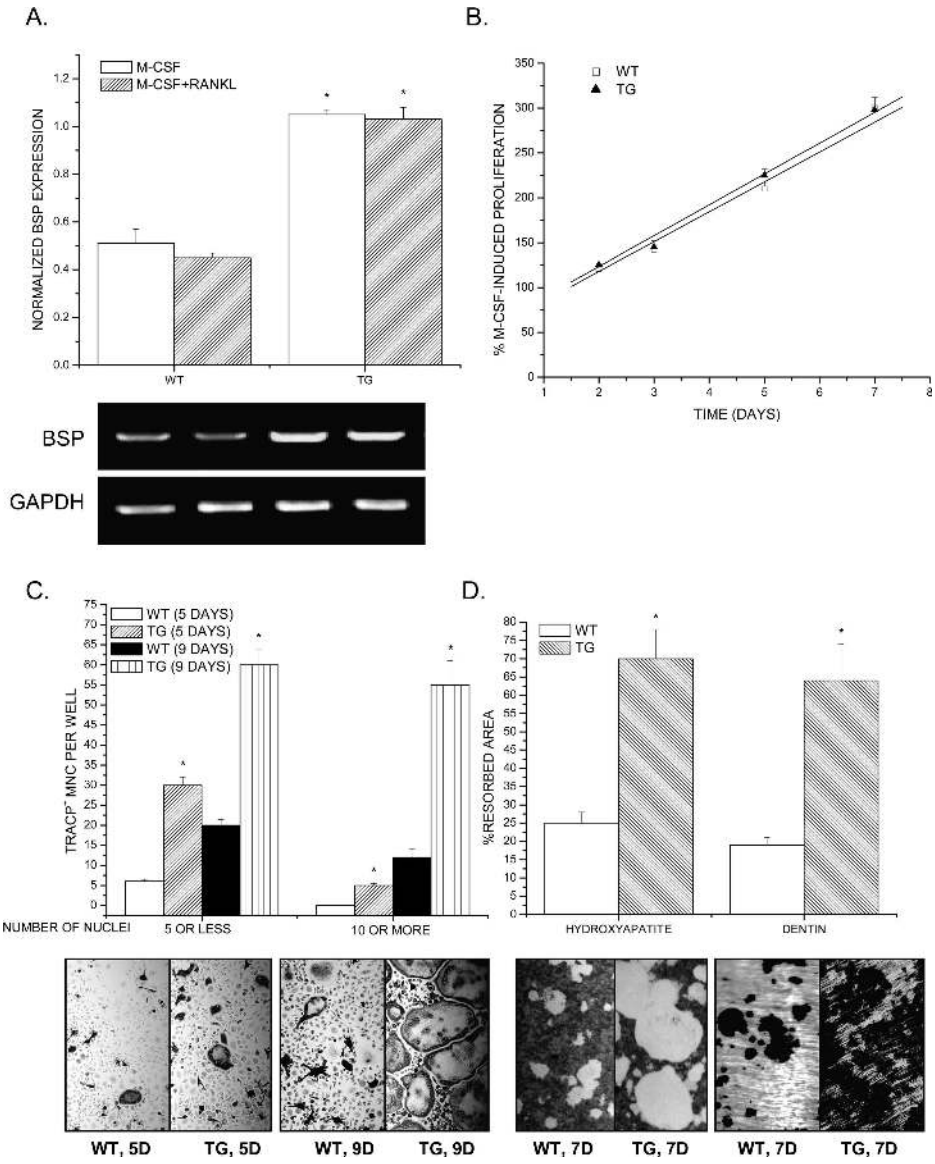

FIG. 4. Analysis of population growth, osteoclast differentiation, and induction of bone resorption pits in vitro by osteoclast-like cells from CMV-BSP transgenic and wildtype mice. (A) BMMs were isolated from 6- to 8-wk-old wildtype (WT) and transgenic mice (TG). Cells were cultured in the presence of 10 ng/ml M-CSF or 10 ng/ml M-CSF and 50 ng/ml RANKL for 5 days and subjected to semiquantitative RT-PCR analysis. Levels of BSP expression were normalized with those of GAPDH. Data are presented as mean ± SE of four different cultures. (*$p <$ 0.01 TG vs. WT at each treatment). (B) Cells were cultured on 96-well plates in the presence of 10 ng/ml M-CSF for different times, and the living cell numbers were determined by MTS assay. (C) Cells were also cultured on 96-well plates in the presence of 10 ng/ml M-CSF and 50 ng/ml RANKL for 5 (5D) or 9 days (9D) to evaluate their differentiation by TRACP staining. Data are presented as mean ± SE of four different cultures. (*$p < 0.01$ TG vs. WT at each time-point). (D) Cells were cultured on hydroxyapatite slices or dentin slices for 7 days (7D) to evaluate their ability to form resorption pits in vitro. Data are presented as mean ± SE of three different cultures. (*$p < 0.01$ TG vs. WT).

more bone nodule formation than those from wildtype mice when the osteogenic differentiation assay was performed on confluent cultures that did not require a proliferative phase to reach confluency. Consistent with a decreased pool of osteoblast caused by lower proliferation rate or higher apoptosis rate in transgenic mice, osteoblast differentiation markers such as ALP activity and OC levels were lower in serum samples of transgenic than in those of wildtype mice. However, the percentage of bone surface covered by cuboidal osteoblast (Ob.S/BS) and the ratio of osteoblast number to bone surface (Ob.N/BS, N/mm) were similar in transgenic mice and wildtype mice, which may be the overall effects of decreased osteoblasts and decreased trabecular bone volume.

Taken together, our findings indicated that BSP overexpression leads to an uncoupling of bone formation and resorption partly because of its effects in enhancing osteoclastic activity and decreasing osteoblast population. These findings were consistent with the recently published paper characterizing the phenotypes of BSP knockout mice. In this paper, Malaval et al.[55] reported that BSP-null mice showed shorter hypomineralized bones, high trabecular bone mass with low turnover rate, impaired bone nodule formation, and retarded osteoclast differentiation. In our CMV-BSP transgenic mice, although decreased cell population in the osteoblast lineage may partly contribute to the decreased BMD of the transgenic mice, the overall effect of BSP overexpression in decreasing bone formation in vivo was not prominent. However, these findings showed that the coupling and balance between bone resorption and bone formation is broken by BSP overexpression in this transgenic mouse model. In agreement with a role of BSP in leading to uncoupled bone resorption and bone formation, histological analysis showed that bones of transgenic mice appeared thinner than those from wildtype mice at different time points. In addition, tibias of transgenic mice showed an

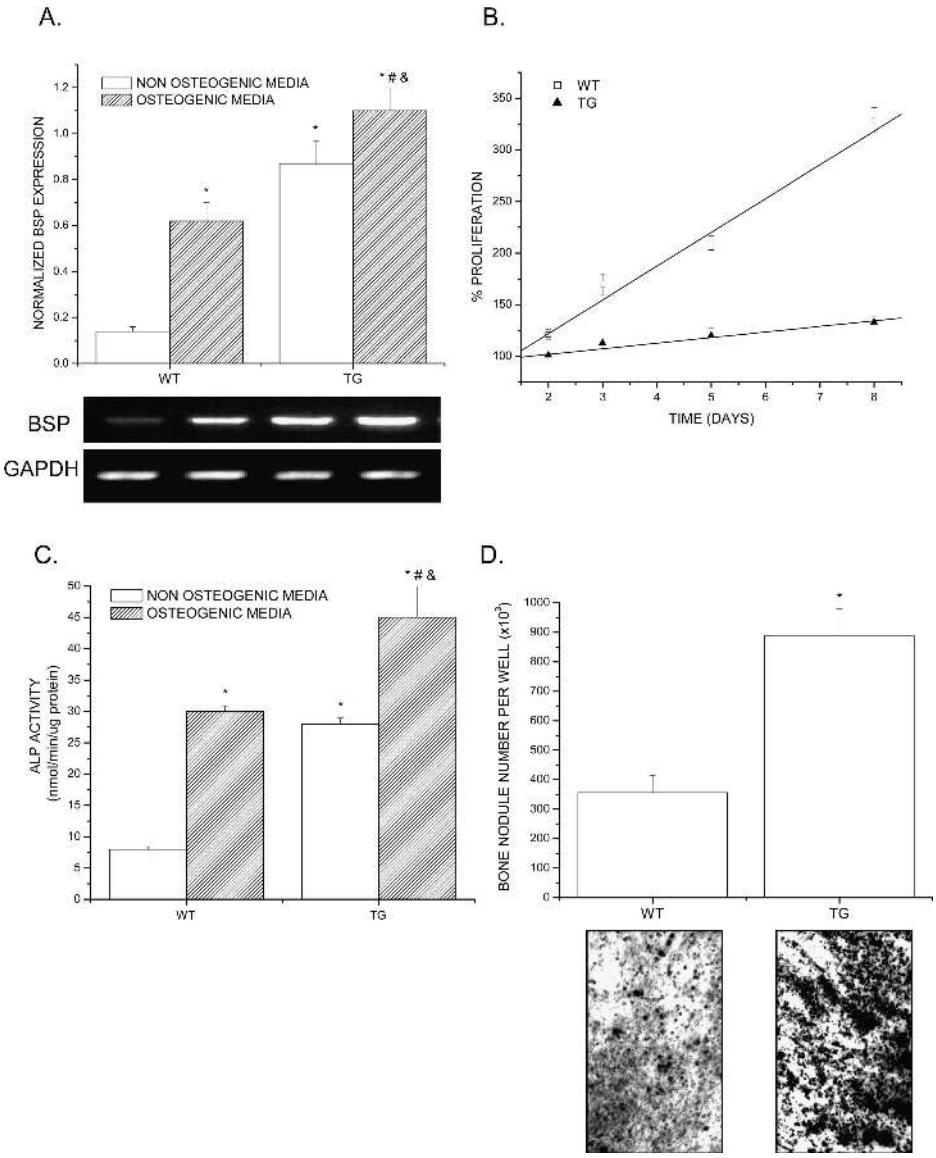

FIG. 5. CMV-BSP calvarial cultures exhibit a lower population growth rate and higher mineralization potential than the cultures derived from wildtype mice in vitro. Calvarial cell cultures isolated from the calvaria of 4-day-old wildtype and transgenic mice were cultured in either osteogenic medium or nonosteogenic medium for 2 wk. (A) Semiquantitative RT-PCR analysis showing the levels of BSP. Levels of BSP expression were normalized with those of GAPDH. Data are presented as mean ± SE of four different cultures. ($^{*}p < 0.01$ vs. WT in nonosteogenic media; $^{\#}p < 0.01$ vs. TG in nonosteogenic media; $^{\&}p < 0.01$ vs. WT in osteogenic media). (B) Population growth rate of cells cultured in nonosteogenic media was determined by the MTS assay. (C) ALP activity of cells cultured in osteogenic or nonosteogenic media. ($^{*}p < 0.01$ vs. WT in nonosteogenic media; $^{\#}p < 0.01$ vs. TG in nonosteogenic media; $^{\&}p < 0.01$ vs. WT in osteogenic media). (D) Alizarin red staining of calvarial cells cultured in osteogenic media for 2 wk. Numbers of bone nodules per well (of 6-well plates) were counted. Data are presented as mean ± SE of four different cultures ($^{*}p < 0.01$, TG vs. WT).

expanded hypertrophic zone at all time points examined and exhibited lower amount of trabecular bone in secondary spongiosa that correlated with a delay in the longitudinal skeletal growth in 6- and 8-wk-old transgenic mice. Because distal hypertrophic chondrocytes need to undergo apoptosis to be replaced by trabecular bone and bone marrow,[56] we speculate that BSP may inhibit this process by inhibiting the apoptosis of the hypertrophic chondrocytes based on our previous findings that BSP inhibits apoptosis in cultures of mature osteoclasts.[21] In addition, the proliferative zone vertical length was decreased in 8-wk-old CMV-BSP mice compared with that in wildtype mice, which indicated that the proliferation of chodrocytes was inhibited in adult transgenic mice.

To summarize, phenotypic analysis of our CMV-BSP transgenic mouse model indicated that BSP overexpression results in the imbalance between bone resorption and bone formation. Our results provide a plausible molecular mechanism for the excessive bone loss observed in a variety of bone pathologies characterized by their high serum levels of BSP and RANKL-to-OPG ratio. In future studies, the CMV-BSP animal model could be used to test whether antibodies against BSP would decrease pathological bone loss and to develop BSP-based therapeutic approaches to treat patients with metabolic bone diseases characterized by their high levels of BSP in serum, which may not be suitable for the available antiresorptive therapies.

ACKNOWLEDGMENTS

This work was supported by National Institutes of Health Grants DE11088 and DE14537 to JC. The authors thank Dr Michael Rosenblatt and members of his laboratory at Tufts Medical School for help with DXA analysis. We also appreciate the comments and suggestions from late Dr Jaro Sodek at University of Toronto for this study.

REFERENCES

1. Frost HM 1990 Skeletal structural adaptations to mechanical usage (SATMU): 1. Redefining Wolff's law: The bone modeling problem. Anat Rec **226:**403–413.
2. Frost HM 1990 Skeletal structural adaptations to mechanical usage (SATMU): 2. Redefining Wolff's law: The remodeling problem. Anat Rec **226:**414–422.
3. Teitelbaum SL 2000 Bone resorption by osteoclasts. Science **289:**1504–1508.
4. Ducy P, Schinke T, Karsenty G 2000 The osteoblast: A sophisticated fibroblast under central surveillance. Science **289:**1501–1504.
5. Akatsu T, Murakami T, Nishikawa M, Ono K, Shinomiya N, Tsuda E, Mochizuki S, Yamaguchi K, Kinosaki M, Higashio K, Yamamoto M, Motoyoshi K, Nagata N 1998 Osteoclastogenesis inhibitory factor suppresses osteoclast survival by interfering in the interaction of stromal cells with osteoclast. Biochem Biophys Res Commun **250:**229–234.
6. Kong YY, Yoshida H, Sarosi I, Tan HL, Timms E, Capparelli C, Morony S, Oliveira-dos-Santos AJ, Van G, Itie A, Khoo W, Wakeham A, Dunstan CR, Lacey DL, Mak TW, Boyle WJ, Penninger JM 1999 OPGL is a key regulator of osteoclastogenesis, lymphocyte development and lymph-node organogenesis. Nature **397:**315–323.
7. Lacey DL, Timms E, Tan HL, Kelley MJ, Dunstan CR, Burgess T, Elliott R, Colombero A, Elliott G, Scully S, Hsu H, Sullivan J, Hawkins N, Davy E, Capparelli C, Eli A, Qian YX, Kaufman S, Sarosi I, Shalhoub V, Senaldi G, Guo J, Delaney J, Boyle WJ 1998 Osteoprotegerin ligand is a cytokine that regulates osteoclast differentiation and activation. Cell **93:**165–176.
8. Yasuda H, Shima N, Nakagawa N, Yamaguchi K, Kinosaki M, Mochizuki S, Tomoyasu A, Yano K, Goto M, Murakami A, Tsuda E, Morinaga T, Higashio K, Udagawa N, Takahashi N, Suda T 1998 Osteoclast differentiation factor is a ligand for osteoprotegerin/osteoclastogenesis-inhibitory factor and is identical to TRANCE/RANKL. Proc Natl Acad Sci USA **95:**3597–3602.
9. Hofbauer LC, Heufelder AE 2001 Role of receptor activator of nuclear factor-kappaB ligand and osteoprotegerin in bone cell biology. J Mol Med **79:**243–253.
10. Theill LE, Boyle WJ, Penninger JM 2002 RANK-L and RANK: T cells, bone loss, and mammalian evolution. Annu Rev Immunol **20:**795–823.
11. Tanaka S, Nakamura K, Takahasi N, Suda T 2005 Role of RANKL in physiological and pathological bone resorption and therapeutics targeting the RANKL-RANK signaling system. Immunol Rev **208:**30–49.
12. Wada T, Nakashima T, Hiroshi N, Penninger JM 2006 RANKL-RANK signaling in osteoclastogenesis and bone disease. Trends Mol Med **12:**17–25.
13. Fisher LW, McBride OW, Termine JD, Young MF 1990 Human bone sialoprotein. Deduced protein sequence and chromosomal localization. J Biol Chem **265:**2347–2351.
14. Chen JK, Shapiro HS, Wrana JL, Reimers S, Heersche JN, Sodek J 1991 Localization of bone sialoprotein (BSP) expression to sites of mineralized tissue formation in fetal rat tissues by in situ hybridization. Matrix **11:**133–143.
15. Chen J, Shapiro HS, Sodek J 1992 Development expression of bone sialoprotein mRNA in rat mineralized connective tissues. J Bone Miner Res **7:**987–997.
16. Paz J, Wade K, Kiyoshima T, Sodek J, Tang J, Tu Q, Yamauchi M, Chen J 2005 Tissue- and bone cell-specific expression of bone sialoprotein is directed by a 9.0 kb promoter in transgenic mice. Matrix Biol **24:**341–352.
17. Tye CE, Rattray KR, Warner KJ, Gordon JA, Sodek J, Hunter GK, Goldberg HA 2003 Delineation of the hydroxyapatite-nucleating domains of bone sialoprotein. J Biol Chem **278:**7949–7955.
18. Wang D, Christensen K, Chawla K, Xiao G, Krebsbach PH, Franceschi RT 1999 Isolation and characterization of MC3T3-E1 preosteoblast subclones with distinct in vitro and in vivo differentiation/mineralization potential. J Bone Miner Res **14:**893–903.
19. Helfrich MH, Nesbitt SA, Dorey EL, Horton MA 1992 Rat osteoclasts adhere to a wide range of RGD (Arg-Gly-Asp) peptide-containing proteins, including the bone sialoproteins and fibronectin, via a beta 3 integrin. J Bone Miner Res **7:**335–343.
20. Flores ME, Norgard M, Heinegard D, Reinholt FP, Andersson G 1992 RGD-directed attachment of isolated rat osteoclasts to osteopontin, bone sialoprotein, and fibronectin. Exp Cell Res **201:**526–530.
21. Valverde P, Tu Q, Chen J 2005 BSP and RANKL induce osteoclastogenesis and bone resorption synergistically. J Bone Miner Res **20:**1669–1679.
22. Ross FP, Chappel J, Alvarez JI, Sander D, Butler WT, Farach-Carson MC, Mintz KA, Robey PG, Teitelbaum SL, Cheresh DA 1993 Interactions between the bone matrix proteins osteopontin and bone sialoprotein and the osteoclast integrin alpha v beta 3 potentiate bone resorption. J Biol Chem **268:**9901–9907.
23. Raynal C, Delmas PD, Chenu C 1996 Bone sialoprotein stimulates in vitro bone resorption. Endocrinology **137:**2347–2354.
24. Razzouk S, Brunn JC, Qin C, Tye CE, Goldberg HA, Butler WT 2002 Osteopontin posttranslational modifications, possibly phosphorylation, are required for in vitro bone resorption but not osteoclast adhesion. Bone **30:**40–47.
25. Bellahcene A, Merville MP, Castronovo V 1994 Expression of bone sialoprotein, a bone matrix protein, in human breast cancer. Cancer Res **54:**2823–2826.
26. Lekic P, Rubbino I, Krasnoshtein F, Cheifetz S, McCulloch CA, Tenenbaum H 1997 Bisphosphonate modulates proliferation and differentiation of rat periodontal ligament cells during wound healing. Anat Rec **247:**329–340.
27. Contri MB, Boraldi F, Taparelli F, De Paepe A, Ronchetti IP 1996 Matrix proteins with high affinity for calcium ions are associated with mineralization within the elastic fibers of pseudoxanthoma elasticum dermis. Am J Pathol **148:**569–577.
28. Diel IJ, Solomayer EF, Seibel MJ, Pfeilschifter J, Maisenbacher H, Gollan C, Pecherstorfer M, Conradi R, Kehr G, Boehm E, Armbruster FP, Bastert G 1999 Serum bone sialoprotein in patients with primary breast cancer is a prognostic marker for subsequent bone metastasis. Clin Cancer Res **5:**3914–3919.
29. Waltregny D, Bellahcene A, Van Riet I, Fisher LW, Young M, Fernandez P, Dewe W, de Leval J, Castronovo V 1998 Prognostic value of bone sialoprotein expression in clinically localized human prostate cancer. J Natl Cancer Inst **90:**1000–1008.
30. Bellahcene A, Maloujahmoum N, Fisher LW, Pastorino H, Tagliabue E, Menard S, Castronovo V 1997 Expression of bone sialoprotein in human lung cancer. Calcif Tissue Int **61:**183–188.
31. Riminucci M, Corsi A, Peris K, Fisher LW, Chimenti S, Bianco P 2003 Coexpression of bone sialoprotein (BSP) and the pivotal transcriptional regulator of osteogenesis, Cbfa1/Runx2, in malignant melanoma. Calcif Tissue Int **73:**281–289.
32. Jung K, Lein M, Stephan C, Von Hosslin K, Semjonow A, Sinha P, Loening SA, Schnorr D 2004 Comparison of 10 serum bone turnover markers in prostate carcinoma patients with bone metastatic spread: Diagnostic and prognostic implications. Int J Cancer **111:**783–791.
33. Fedarko NS, Jain A, Karadag A, Van Eman MR, Fisher LW 2001 Elevated serum bone sialoprotein and osteopontin in colon, breast, prostate, and lung cancer. Clin Cancer Res **7:**4060–4066.
34. Shaarawy M, Hasan M 2001 Serum bone sialoprotein: A marker of bone resorption in postmenopausal osteoporosis. Scand J Clin Lab Invest **61:**513–521.
35. Seibel MJ, Woitge HW, Pecherstorfer M, Karmatschek M, Horn E, Ludwig H, Armbruster FP, Ziegler R 1996 Serum immunoreactive bone sialoprotein as a new marker of bone turnover in metabolic and malignant bone disease. J Clin Endocrinol Metab **81:**3289–3294.

36. Saxne T, Zunino L, Heinegard D 1995 Increased release of bone sialoprotein into synovial fluid reflects tissue destruction in rheumatoid arthritis. Arthritis Rheum **38:**82–90.
37. Acebes C, de la Piedra C, Traba ML, Seibel MJ, Garcia Martin C, Armas J, Herrero-Beaumont G 1999 Biochemical markers of bone remodeling and bone sialoprotein in ankylosing spondylitis. Clin Chim Acta **289:**99–110.
38. Stork S, Stork C, Angerer P, Kothny W, Schmitt P, Wehr U, von Schacky C, Rambeck W 2000 Bone sialoprotein is a specific biochemical marker of bone metabolism in postmenopausal women: A randomized 1-year study. Osteoporos Int **11:**790–796.
39. Woitge HW, Oberwittler H, Heichel S, Grauer A, Ziegler R, Seibel MJ 2000 Short- and long-term effects of ibandronate treatment on bone turnover in Paget disease of bone. Clin Chem **46:**684–690.
40. Xiao Z, Awad HA, Liu S, Mahlios J, Zhang S, Guilak F, Mayo MS, Quarles LD 2005 Selective Runx2-II deficiency leads to low-turnover osteopenia in adult mice. Dev Biol **283:**345–356.
41. Modric T, Silha JV, Shi Z, Gui Y, Suwanichkul A, Durham SK, Powell DR, Murphy LJ 2001 Phenotypic manifestations of insulin-like growth factor-binding protein-3 overexpression in transgenic mice. Endocrinology **142:**1958–1967.
42. Tu Q, Pi M, Karsenty G, Simpson L, Liu S, Quarles LD 2003 Rescue of the skeletal phenotype in CasR-deficient mice by transfer onto the Gcm2 null background. J Clin Invest **111:**1029–1037.
43. Park BK, Zhang H, Zeng Q, Dai J, Keller ET, Giordano T, Gu K, Shah V, Pei L, Zarbo RJ, McCauley L, Shi S, Chen S, Wang CY 2007 NF-kappaB in breast cancer cells promotes osteolytic bone metastasis by inducing osteoclastogenesis via GM-CSF. Nat Med **13:**62–69.
44. Bellows CG, Ciaccia A, Heersche JN 1998 Osteoprogenitor cells in cell populations derived from mouse and rat calvaria differ in their response to corticosterone, cortisol, and cortisone. Bone **23:**119–125.
45. Galli M, Nuti R, Franci B, Righi G, Martorelli MT, Turchetti V, Caniggia M 1985 Serum osteocalcin radioimmunoassay in bone diseases. Ric Clin Lab **15:**253–257.
46. Gundberg CM, Markowitz ME, Mizruchi M, Rosen JF 1985 Osteocalcin in human serum: A circadian rhythm. J Clin Endocrinol Metab **60:**736–739.
47. Halleen JM, Alatalo SL, Suominen H, Cheng S, Janckila AJ, Vaananen HK 2000 Tartrate-resistant acid phosphatase 5b: A novel serum marker of bone resorption. J Bone Miner Res **15:**1337–1345.
48. Lees RL, Sabharwal VK, Heersche JN 2001 Resorptive state and cell size influence intracellular pH regulation in rabbit osteoclasts cultured on collagen-hydroxyapatite films. Bone **28:**187–194.
49. Murshed M, Harmey D, Millan JL, McKee MD, Karsenty G 2005 Unique coexpression in osteoblasts of broadly expressed genes accounts for the spatial restriction of ECM mineralization to bone. Genes Dev **19:**1093–1104.
50. Hakki SS, Wang D, Franceschi RT, Somerman MJ 2006 Bone sialoprotein gene transfer to periodontal ligament cells may not be sufficient to promote mineralization in vitro or in vivo. J Periodontol **77:**167–173.
51. Wang J, Zhou HY, Salih E, Xu L, Wunderlich L, Gu X, Hofstaetter JG, Torres M, Glimcher MJ 2006 Site-specific in vivo calcification and osteogenesis stimulated by bone sialoprotein. Calcif Tissue Int **79:**179–189.
52. Singer FRRG 1996 Paget's disease. In: Bilezikian J, Raisz L, Rodan G (eds.) Principles of Bone Biology. Academic Press, San Diego, CA, USA, pp. 969–977.
53. Kaye M, Zucker SW, Leclerc YG, Prichard S, Hodsman AB, Barre PE 1985 Osteoclast enlargement in endstage renal disease. Kidney Int **27:**574–581.
54. Makris GP, Saffar JL 1982 Quantitative relationship between osteoclasts, osteoclast nuclei and the extent of the resorbing surface in hamster periodontal disease. Arch Oral Biol **27:**965–969.
55. Malaval L, Wade-Gueye NM, Boudiffa M, Fei J, Zirngibl R, Chen F, Laroche N, Roux JP, Burt-Pichat B, Duboeuf F, Boivin G, Jurdic P, Lafage-Proust MH, Amedee J, Vico L, Rossant J, Aubin JE 2008 Bone sialoprotein plays a functional role in bone formation and osteoclastogenesis. J Exp Med **205:**1145–1153.
56. Gibson G 1998 Active role of chondrocyte apoptosis in endochondral ossification. Microsc Res Tech **43:**191–204.

Address reprint requests to:
Qisheng Tu, MD, PhD
Jake Chen, DDS, PhD
Division of Oral Biology
Tufts University School of Dental Medicine
One Kneeland Street
Boston, MA 02111, USA
E-mail: qisheng.tu@tufts.edu; jk.chen@tufts.edu

Received in original form December 21, 2007; revised form June 4, 2008; accepted June 27, 2008.